A 3-Dimensional Finite Element Analysis of Adjacent Segment Disk Degeneration Induced by Transforaminal Lumbar Interbody Fusion After Pedicle Screw Fixation

Tuan-Mao Guo, Jian Lu, Yan-Li Xing, Guo-Xiong Liu, Hai-Yun Zhu, Lan Yang, Xi-Min Qiao

■ BACKGROUND: **Transforaminal lumbar interbody fusion (TLIF) is an effective treatment of upper lumbar intervertebral disk herniation. However, its clinical efficacy for adjacent segment disk degeneration (ASDD) remains undefined. Therefore, the biomechanical evaluation of ASDD caused by TLIF after pedicle screw fixation (PSF) was explored via a 3-dimensional (3D) finite element analysis.**

■ METHODS: **Computed tomography images of a healthy male adult volunteer were used in this study. A L3-4 3D finite element model (model) was successfully constructed using Pro/E software, which was also used to establish the L4-5 of the TLIF, PSF, and PSF + TLIF models. Under the same loading conditions, the protrusion and retraction of the adjacent intervertebral disk and the stress distribution of the annulus fibrosis, facet joint, and articular process in the TLIF, PSF, and PSF + TLIF models were all compared.**

■ RESULTS: **Protrusion and retraction of the adjacent intervertebral disk were more notable in the PSF + TLIF model than in the PSF model under the same loading conditions. The stress of the annulus fibrosis of the PSF + TLIF model was stronger relative to that of the PSF model under flexion, extension, or lateral bending. The stress of the articular process of the PSF + TLIF model was also stronger than that of the PSF model under extension or lateral bending.**

■ CONCLUSIONS: **This study provides evidence that TLIF may aggravate ASDD after PSF. Furthermore, the findings provided in this report represent the theoretic basis for the clinical analysis of ASDD caused by TLIF after PSF.**

INTRODUCTION

The intervertebral disks in human bodies serve as shock absorbers between vertebrae, whereas paired facet joints are responsible for refraining from motion. These joints can eventually become incompetent, enabling one vertebral body to slip forward onto the other as they age. This slipping of vertebral bodies can lead to friction among vertebral bodies.[1] Often viewed as a multifactorial and heterogeneous process, intervertebral disk degeneration mainly has negative effects on the working population, functioning as a major contributor to lower back pain.[2,3] The pathogenesis of intervertebral disk degeneration involves an extremely complex, extensive, and poorly understood process, by which many different genetic, biological, and mechanical factors apply tremendous influence on the breakdown of extracellular matrix components.[4] Because of this, anytime mechanical conditions become abnormal, regardless of altered nutrition, an upset of the homeostasis in intervertebral disk degeneration will occur. Because of the change in homeostasis in the intervertebral tissue damage, adaptive changes will occur, thereby initiating or even accelerating degenerative changes of the biochemical composition and structure of intervertebral disk degeneration.[5]

A common treatment option for patients suffering from intervertebral disk degeneration is transforaminal lumbar interbody fusion (TLIF), a technique for diverse disorders in lumbar

Key words
- 3-dimensional finite element analysis
- Adjacent segment disk degeneration
- Annulus fibrosis
- Biomechanical study
- Intervertebral disk
- Transforaminal lumbar interbody fusion

Abbreviations and Acronyms
3D: 3-Dimensional
ANOVA: Analysis of variance
ASDD: Adjacent segment disk degeneration
NP: Nucleus pulposus
PLIF: Posterior lumbar interbody fusion
PSF: Pedicle screw fixation
TLIF: Transforaminal lumbar interbody fusion

Department of Orthopedics, Xianyang Central Hospital, Xianyang, P.R. China

To whom correspondence should be addressed: Xi-Min Qiao, M.M. [E-mail: gtm0619@163.com]

Tuan-Mao Guo and Jian Lu are co–first authors.

Citation: World Neurosurg. (2019) 124:e51-e57.
https://doi.org/10.1016/j.wneu.2018.11.195

*Journal homepage: **www.journals.elsevier.com/world-neurosurgery***

*Available online: **www.sciencedirect.com***

1878-8750/$ - see front matter

degeneration for more than 30 years.[6] Developed as a modification of posterior lumbar interbody fusion (PLIF), TLIF represents a unilateral and direct approach to the intervertebral foraminal area, while avoiding destruction of the anatomic integrity of the spinal neural elements.[7] The TLIF procedure boasts the advantages of low risks and low incidences of radiculitis postoperation, and patients receiving TLIF can recover quickly.[8] It has been demonstrated that TLIF could be used to treat patients suffering from lumbar intervertebral disk herniation together with instable spine.[9] Despite the advantages previously mentioned, TLIF has also been associated with complications, including intraoperative neurologic injury, infection, osteolysis, and heterotopic ossification.[10] More specifically, it was found that adjacent segment disk degeneration (ASDD) remains one of the long-term complications in patients post-TLIF.[11] However, it is still unknown as to how TLIF is directly associated with ASDD. At the moment, many researchers have turned to biomechanical testing and finite element analysis methods for closer studies involving intervertebral disk degeneration and have yielded rewarding results.[12,13] Furthermore, combined treatment of TLIF (with single cage) and unilateral pedicle screw fixation (PSF) could benefit people suffering from lumbar instability by contributing to reduced trauma, lower blood loss, reduced economic cost, and faster recovery.[14] Overall, this study intends to evaluate the biomechanical effects TLIF has on ASDD using a 3-dimensional (3D) finite element analysis involving the aid of biomechanical testing in the hopes of instructing a clinical decision on the treatment of intervertebral disk degeneration and the complication of ASDD after TLIF.

MATERIALS AND METHODS

Ethics Statement

This study was conducted based on the principle of voluntary participation and was in accordance with the protocols proposed by the committee of our hospital (number XY2018LL013). The patient involved in this study signed written informed consent prior to the study. The participant knew well about the study prior to the experiment and had the capability to complete all plans.

Establishment of the Finite Element Model of the Lumbar Spine

A young male volunteer with no history of pain in the waist or trauma was selected to take part in this study and received radiograph scanning. The volunteer stood at a height of 172 cm and weighed 68 kg. The radiograph showed no deformity or disk degeneration in his lumbar spine. The scanning was conducted with the parameters of 80 kV and 250 mA, and the patient was posed in the supine position. The scanning table was adjusted to locate the scanning area, with the L3-5 spinal segments being observed with a scanning thickness of 1 mm. The images were obtained and saved with the form of digital imaging and communications in medicine. The final 2-dimensional images were obtained with effect noise on the computed tomography image, and unnecessary bone area was excluded. This was followed by editing and removal procedures on the images using mask tools for the full and clear presentation of the image margin. With the image margin now full and clear for observation, the 3D model (model) images were obtained. Pro/E software and other instruments, including 4 Reco pedicle screws (diameter, 4.5 mm; length, 60 mm), 2 Reco titanium connecting rods (diameter, 6.0 mm; length, 70 mm), and a cage fusion, were all applied to simulate a spinal internal fixation system (SofamorDanek, Memphis, Tennessee, USA). The 3D images were then inputted into the Mimics.3.0 software (Materialise, Heverlee, Belgium) in the form of stereolithography. The screw rod fixation system and lumbar spine were successfully established, simplified, and adjusted. Intervertebral disk and the ligaments in the lumbar spine were also added based on the bony structure. Finally, the results from the data were inputted in Hypermesh (Altair, Troy, Michigan, USA) for model establishment.

Parameters for the Finite Element Model

The 6-node triangular thin shell elements were used to simulate cortical bone with a thickness of 1 mm. A model based on the terminal plate of the vertebral body, cancellous bone, matrix, and posterior structure of the intervertebral disk was established. This model also included the annulus fibrosis and 10-node tetrahedrons, such as the radix arcus vertebrae, terminal plate, isthmus, spinous process, facet joints, and transverse process. The pulposus was simulated as an incompressible elastic amount of fluids, composed of node solid units. The surface on the articular cartilage layer was conducted using frictionless sliding surface interface elements. The initial distance between the interface elements was 0.6 mm, and the friction index was 0. The material belonging to the arthrodial cartilage was linearly elastic with the modulus elasticity setting at 10,000 Pa. The anterior longitudinal, posterior longitudinal, supra interspinous, interspinal, posterolateral ligament, ligamentum flavum, and capsules of the finite element model were all simulated using an abundance of elastic cable elements. The position of the element, cross-sectional area, and its length were all based on the actual anatomic structure (Table 1).

Establishment of the TLIF Model

The TLIF model was established based on the preceding finite element model. To begin with, the TLIF model was performed to the stimulation of titanium alloy PSF with the Sextant system (Medtronic Inc., Minneapolis, MN, USA), with a screw diameter of 6.5 mm, length of 50 mm, Young modulus of 110,000 MPa, and Poisson ratio of 0.3. The pedicle screws were contacted with bony structures using the binding method (PSF model). Posterior laminectomy was performed on the L4-5 segments based on the PSF model. Cage fusion and radix arcus vertebrae screws were applied for fixation (PSF + TLIF model).

Index Evaluation

The biomechanical degrees of freedom, which were presented on the lower surface and inferior articular surface on the L5 segment from XYZ directions, were terminated in the case of translation and torsions. The L3 segment was physiologically loaded with 500 N and 15 Nm and was also added to simulate the activities of flexion, extension, left bending, right bending, left rotation, and right rotation of the human lumbar vertebra. The protrusions and retractions of the lumbar vertebra were recorded and compared between both the PSF and PSF + TLIF models under the same conditions and stresses on the annulus

Table 1. Property of the Materials for the Finite Element Model

Element	Unit Type	Unit Number	Modulus of Elasticity (MPa)	Poisson Ratio	Cross-Sectional Area (mm^2)
Vertebral cortical bone	6-node shell element	10,096	12,000	0.3	
Vertebral cancellous bone	10-node solid element	67,747	100	0.2	
Terminal plate of vertebral body	10-node solid element	2064	1000	0.25	
Matrix structure of anulus fibrosus	10-node solid element	20,679	4.2	0.45	
Anterior longitudinal ligament	2-node cable element	9	20	0.3	759
Posterior longitudinal ligament	2-node cable element	5	20	0.3	518
Ligamentum flavum	2-node cable element	6	19.5	0.3	787
Posterolateral ligament	2-node cable element	6	50	0.3	20
Capsules	2-node cable element	10	20	0.3	1025
Interspinal ligament	2-node cable element	10	28	0.3	363
Supra interspinous ligament	2-node cable element	4	28	0.3	757
Fusion cage	10-node solid element	3980	3700	0.25	
Radix arcus vertebrae screw	10-node solid element	7860	110,000	0.3	

fibrosis, facet joints, and articular process. The von Mises stress on the 10 nodes in the left and right facet joints was selected to calculate the mean fusion stress on each node under various loading stress.[15,16]

Statistical Analysis

SPSS version 13.0 (SPSS Inc., Chicago, Illinois, USA) was used for data analysis. All data were displayed under mean ± SD. One-way analysis of variance (ANOVA) was used to compare data between groups. Pairwise comparisons were conducted using Newman-Keuls test. $P < 0.05$ was set as the standard to show significant difference.

RESULTS

PSF and PSF + TLIF Models Are Successfully Constructed

The finite element model (L3-5) was successfully established using a total of 110,421 elements. TLIF was successfully simulated based on the PSF and PSF + TLIF models (Figure 1).

Adjacent Intervertebral Disk in the PSF + TLIF Model Is Obviously Bulged and Invaginated

After undergoing stress from all the simulated activities, the intervertebral disk at the tension side was centripetally invaginated, while a radial bulge was observed at the squeezed site. The intervertebral disk was radiated, maximizing to the posterior margin when squeezed; meanwhile, the anterior and posterior margins of the intervertebral disk had maximum invagination under flexion and extension. When undergoing stress from simulated lateral flexion, the posterior-lateral margin of the intervertebral disk bore its maximum bulge. While under a twisting motion, the intervertebral disk distorted correspondingly with the motion of the upper vertebral body, and the posterior-lateral margin of the intervertebral disk bore the maximum deformation. Compared with that of the model, the adjacent intervertebral disk was highly bulged and invaginated in the PSF and PSF + TLIF models, especially in the PSF + TLIF model (both $P < 0.05$) (Figure 2A and B).

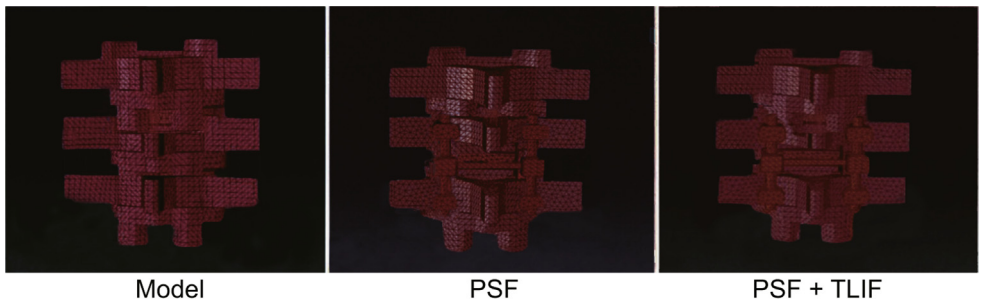

Figure 1. Finite element model, pedicle screw fixation model, and pedicle screw fixation + transforaminal lumbar interbody fusion model were successfully constructed using a total of 110,421 elements. Model, finite element model; PSF, pedicle screw fixation; TLIF, transforaminal lumbar interbody fusion.

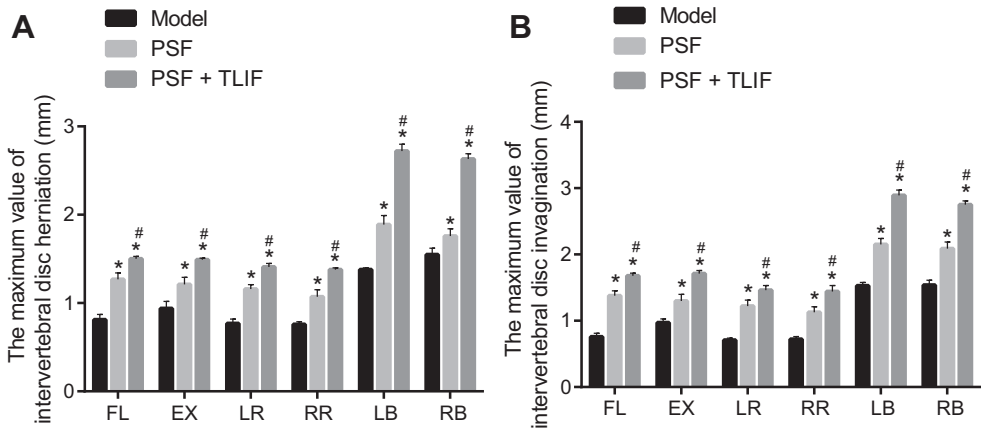

Figure 2. The pedicle screw fixation + transforaminal lumbar interbody fusion model demonstrates increased bulge and invagination of the adjacent intervertebral disk under different stress loading: (**A**) the maximum value (millimeters) of bulge of the adjacent intervertebral disk under different stress loading (n = 10) and (**B**) the maximum value (millimeters) of invagination of the adjacent intervertebral disk under different stress loading (n = 10). *$P < 0.05$ vs. model; #$P < 0.05$ vs. the pedicle screw fixation model. The results were measurement data; the 1-way analysis of variance was performed for multiple-group comparison. EX, extension; FL, flexion; LB, left bending; LR, left rotation; PSF, pedicle screw fixation; RB, right bending; RR, right rotation; TLIF, transforaminal lumbar interbody fusion.

PSF + TLIF Model Illustrates Enhanced Stress on the Annulus Fibrosis of the Adjacent Intervertebral Disk

With the size and invagination rate of the intervertebral disk now fully established and examined, the next step in this experiment was to examine the stress rate the PSF + TLIF model had on the adjacent intervertebral disk. While undergoing stress loading, the maximum tensile stress of the annulus fibrosis was shown to be well-distributed. The stretch side of the intervertebral disk included the site of maximum tensile stress under 15 Nm going through lateral, bending, and flexion movement. The posterior fiber of the intervertebral disk bore the maximum tensile stress under flexion, whereas the anterior fiber of the intervertebral disk bore the maximum tensile stress under extension. When lateral bending was performed in the stretched side, maximum tensile stress was located in the posterior lateral region. The left or right posterior lateral regions in the stretched side bore the maximum tensile stress when right or left lateral bending was performed. Torsional movement resulted in maximum tensile stress on the posterior lateral region of the opposite direction ($P < 0.05$). The tensile stress was significantly altered in the PSF and PSF + TLIF models ($P < 0.05$). Under the condition of 15-Nm torsional movements, the PSF and PSF + TLIF models exhibited maximum tensile stress, when compared with that of the model, and further increased in the PSF + TLIF model compared with that in the PSF model ($P < 0.05$) (Figure 3).

Stress Distribution Changes at the Adjacent Facet Joints

With the stress rate of the PSF + TLIF model established, and its effects on the annulus fibrosis of the adjacent intervertebral disk fully examined, the subsequent step in this experiment was to examine and draw an understanding of the stress distribution changes that occur at the adjacent facet joints. To begin, the load values of the facet joints, and stress distribution of the articular cartilage, were accordingly altered with the change during load from activities. The maximum load value of facet joints was from torsion and extension, followed by lateral bending and flexion. The load value of the facet joints and the stress of articular cartilage were relatively higher in the opposite direction of the torsion, while also bearing no stress from the torsion side. During extension, the stress-bearing area changed from the articular cartilage to the superior articular inferior part, whereas the superior articular upper part bore maximum tensile stress and facet joints bore lower stress under flexion. Under lateral bending, both sides of the facet joints bore stress; however, the maximum tensile stress was found at the superior articular upper part of the same bending side and the superior articular inferior part of the

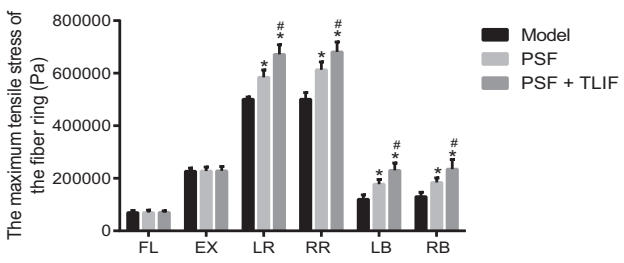

Figure 3. The maximum tensile stress (pascals) of the annulus fibrosis under different stress loading (n = 10). *$P < 0.05$ vs. model; #$P < 0.05$ vs. the pedicle screw fixation model. The results were measurement data; the 1-way analysis of variance was performed for multiple-group comparison. EX, extension; FL, flexion; LB, left bending; LR, left rotation; PSF, pedicle screw fixation; RB, right bending; RR, right rotation; TLIF, transforaminal lumbar interbody fusion.

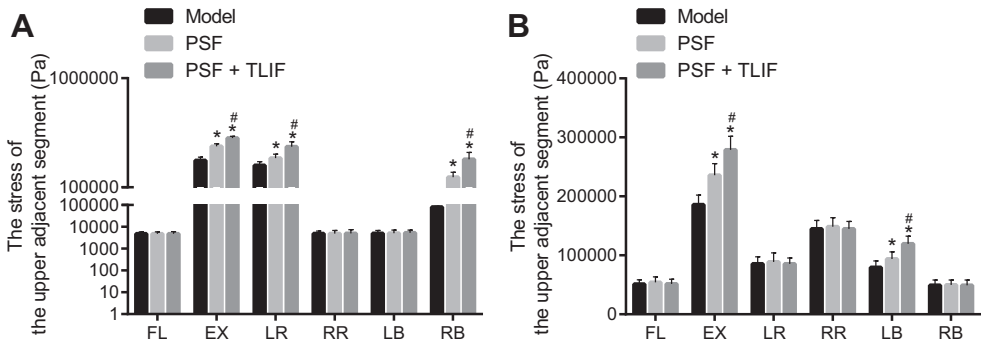

Figure 4. Distribution of equivalent stress on the articular process was higher in the pedicle screw fixation + transforaminal lumbar interbody fusion model. (**A**) The equivalent stress on the articular process on L3 with 500-N loading (n = 10). (**B**) The equivalent stress on the articular process on L3 with 50-Nm extension stress (n = 10). *$P < 0.05$ vs. model; #$P < 0.05$ vs. the pedicle screw fixation model. The results were measurement data; the 1-way analysis of variance was performed for multiple-group comparison. EX, extension; FL, flexion; LB, left bending; LR, left rotation; PSF, pedicle screw fixation; RB, right bending; RR, right rotation; TLIF, transforaminal lumbar interbody fusion.

opposite bending side. The overall stress bore from both sides of the facet joints in the TLIF model showed no significant differences under load from all the activities ($P > 0.05$) (Figure 4).

Distribution of Equivalent Stress on the Articular Process and Superior Adjacent Segment Was Higher in the PSF + TLIF Model

With the stress distribution at the adjacent facet joints now established and fully studied, the next step was to examine the distribution of equivalent stress on the articular process and to study the superior adjacent segment in the PSF + TLIF model. To do this, the stress distribution on the superior adjacent articular process was first studied, which can be seen in Figure 4A and B. No significant difference was found between compression or flexion when equivalent stress of the superior adjacent articular process was distributed (both $P > 0.05$). The equivalent stress in the PSF and PSF + TLIF models was significantly higher than that of the model in extension, and further increased in the PSF + TLIF model when compared with that of the PSF model ($P < 0.05$), while showing no significant difference on equivalent stress of opposite sides ($P > 0.05$). No significant differences were examined on the equivalent stress of torsion sides among the model and the PSF and PSF + TLIF models ($P > 0.05$), whereas equivalent stress of the opposite side during torsion in the PSF and PSF + TLIF models was higher than that of the model, and further increased in the PSF + TLIF model when compared with that of the PSF model ($P < 0.05$). The articular process in the PSF and PSF + TLIF models showed a significant equivalent stress during extension (Figure 5).

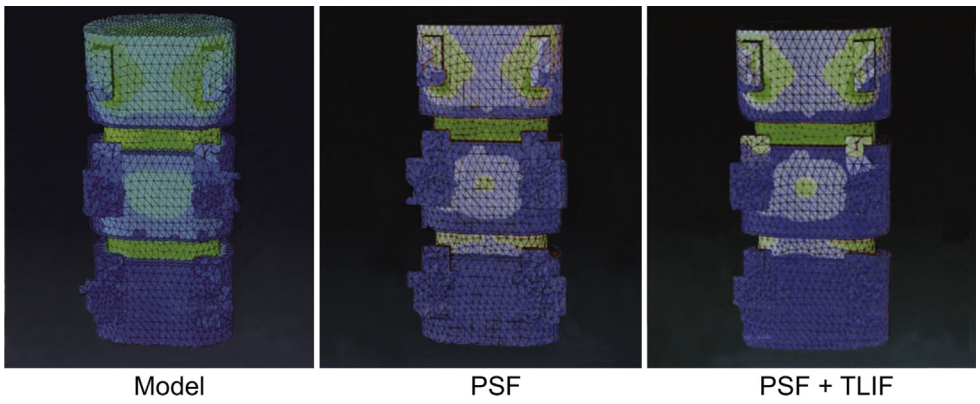

Figure 5. The equivalent stress on the articular process on L3 with 500-N loading and 50-Nm extension stress in the pedicle screw fixation and pedicle screw fixation + transforaminal lumbar interbody fusion models. Stress concentration was presented in both the pedicle screw fixation and pedicle screw fixation + transforaminal lumbar interbody fusion models. Model, finite element model; PSF, pedicle screw fixation; TLIF, transforaminal lumbar interbody fusion.

DISCUSSION

Despite the high success rate of the TLIF technique, it is undeniable that it can lead to some complications and risks, such as ASDD.[10,11] Moreover, it still remains unclear in what way TLIF leads to ASDD, with the objective of this experiment set to explore specific changes after TLIF to investigate the association between TLIF and ASDD.

This study revealed that, based on 3D finite element modeling, the PSF + TLIF model showed a more notable bulge and invagination compared with that of the PSF model, indicating TLIF's association with ASDD. Given the overwhelming difficulties regarding the in vivo study of cellular activity and nutrient distributions, especially in human disks, finite element modeling of the disk can help to better understand the in vivo environment.[12] Yan et al.[17] discovered that clinically relevant symptomatic adjacent segment disease was present at an average of 26.8 months, whereas lumbar fusion increased the incidence rate of ASDD from about 5% to 43%, an increase greater than 800%. Biomechanical and clinical studies uncovered certain discoveries, including that spinal fusion initiates a remarkable, compensatory increase in motion in the adjacent mobile segments because of an increase of stiffness of the fused segment.[18] After fusion, the neighboring unfused segments must move with great frequencies toward the upper limits of their functional ranges of motion. This is done to compensate for the alterations in the spinal alignment and the spinal motions lost at the fused segments to keep an erect posture and the center of gravity at stable levels.[19] Because of this, there is a high possibility that the postoperative lumbar alignment speeds up adjacent segment deterioration by putting too much load on the motion segments than can handle the capacity,[20] thereby potentially giving rise to the adjacent intervertebral disk degeneration. When the adjacent intervertebral disk degenerates, changes in the biochemical and structural components will ensue, leading to progressive loss of proteoglycan content. Continuing with the subsequent events after the degeneration of the adjacent intervertebral disk, dehydration of the nucleus pulposus (NP) will occur, followed by a decline of hydrostatic pressure in the disk ensued by impaired load bearing,[5] making the adjacent disk too stiff to return to normal after compression. Lee and Langrana[21] reported similar results to the findings found in this report, with all types of fusion (including posterior fusion) potentially leading to an increased bending and axial stiffness, further in relation with our findings.

Moreover, while conducting this study, it was also found that the PSF + TLIF model notably demonstrated increased stress on the annulus fibrosis and articular process compared with that of the PSF model. Xu et al.[22] have previously conducted a study to compare the biomechanical difference between PLIF and TLIF using a finite element analysis, finding that the TLIF approach could contribute to biomechanical stability and decrease stress at the cage–end plate interface and could rescue the shortcomings of the PLIF technique. The specific compartments of the disk, including the NP, annulus fibrosis, transition zone between the NP and annulus fibrosis, and the vertebral end plates and extracellular matrix, combine to serve as a multiaxial, hydrophilic, viscoelastic, and flexible joint between vertebrae.[13] Nonetheless, during disk degeneration, the proteolytic actions of matrix metalloproteinases and aggrecanases responsible for the breakdown of several matrix components displayed an increase, which further induces a decrease in the extracellular matrix.[4] When observing the ensuing changes in the extracellular matrix components, mechanical functions of the tissues are likely to be influenced.[2] Therefore, compared with nondegenerative NP at the fusion site, which is more fluid-like with a high content of water, degenerative NP at adjacent sites seems more fibrous with inferior hydrophilic properties, therefore turning into a more solid-like structure.[23] A result consistent with the findings in this report was shared by Lee,[24] who was specific about spinal fusion procedures on adjacent segments, indicating an obvious increase in degree of stress at that segment, further supporting this study.

CONCLUSIONS

Based on finite element modeling, TLIF is likely to incur ASDD after the operation in hopes of instructing clinical analysis of the troublesome complication. However, this study also has its own limitations. Because the study was carried out on models rather than on human bodies, and given our more complicated structure, we have a long way to go before we can apply this procedure on human beings for our desired results. Also, the present models did not account for the mechanical effect of muscle contraction, and the loading conditions were not truly physiologic, which may not be completely representative of the clinical situation. Besides, the study was based on 1 case and may result in incomprehensive conclusions, and more efforts will be made to conduct more comprehensive exploration with larger sample sizes in the near future. Furthermore, similar studies should be conducted with clinical data to obtain more proof of our concept using the computed tomography scans of patients with disease in various age groups.

ACKNOWLEDGMENTS

The authors would like to give our sincere appreciation to the reviewers for their helpful comments on this article.

REFERENCES

1. Taghiabadi E, Mohammadi P, Aghdami N, et al. Treatment of hypertrophic scar in human with autologous transplantation of cultured keratinocytes and fibroblasts along with fibrin glue. *Cell J.* 2015;17:49-58.
2. Turgut M, Basaloglu HK, Yenisey C, Ozsunar Y. Surgical pinealectomy accelerates intervertebral disc degeneration process in chicken. *Eur Spine J.* 2006;15:605-612.
3. Millecamps M, Tajerian M, Naso L, Sage EH, Stone LS. Lumbar intervertebral disc degeneration associated with axial and radiating low back pain in ageing SPARC-null mice. *Pain.* 2012;153:1167-1179.
4. Tiaden AN, Klawitter M, Lux V, et al. Detrimental role for human high temperature requirement serine protease A1 (HTRA1) in the pathogenesis of intervertebral disc (IVD) degeneration. *J Biol Chem.* 2012;287:21335-21345.
5. Kim J, Yang SJ, Kim H, et al. Effect of shear force on intervertebral disc (IVD) degeneration: an in vivo rat study. *Ann Biomed Eng.* 2012;40:1996-2004.
6. Tian NF, Wu YS, Zhang XL, Xu HZ, Chi YL, Mao FM. Minimally invasive versus open

transforaminal lumbar interbody fusion: a meta-analysis based on the current evidence. *Eur Spine J*. 2013;22:1741-1749.

7. Villavicencio AT, Burneikiene S, Roeca CM, Nelson EL, Mason A. Minimally invasive versus open transforaminal lumbar interbody fusion. *Surg Neurol Int*. 2010;1:12.

8. Yan DL, Pei FX, Li J, Soo CL. Comparative study of PILF and TLIF treatment in adult degenerative spondylolisthesis. *Eur Spine J*. 2008;17:1311-1316.

9. Wang L, Liu C, Li GQ, Tian JW. [Transforaminal lumbar interbody fusion in the treatment of lumbar intervertebral disc herniation with lumbar instability] [in Chinese]. *Zhonghua Yi Xue Za Zhi*. 2012;92:2781-2784.

10. Chrastil J, Patel AA. Complications associated with posterior and transforaminal lumbar interbody fusion. *J Am Acad Orthop Surg*. 2012;20:283-291.

11. Bae JS, Lee SH, Kim JS, Jung B, Choi G. Adjacent segment degeneration after lumbar interbody fusion with percutaneous pedicle screw fixation for adult low-grade isthmic spondylolisthesis: minimum 3 years of follow-up. *Neurosurgery*. 2010;67:1600-1607 [discussion: 1607-1608].

12. Jackson AR, Huang CY, Brown MD, Gu WY. 3D finite element analysis of nutrient distributions and cell viability in the intervertebral disc: effects of deformation and degeneration. *J Biomech Eng*. 2011;133:091006.

13. Erwin WM, DeSouza L, Funabashi M, et al. The biological basis of degenerative disc disease: proteomic and biomechanical analysis of the canine intervertebral disc. *Arthritis Res Ther*. 2015;17:240.

14. Hua YJ, Wang RY, Guo ZH, Zhu LM, Lu JY. [Treatment of lumbar instability with transforaminal lumbar interbody fusion (with single cage) combined with unilateral pedicle screw fixation] [in Chinese]. *Zhongguo Gu Shang*. 2014;27:722-725.

15. Shin JK, Goh TS, Kim M-S, et al. Stress and strain analyses of single and segmental lumbar spines based on an accurate finite element model for vertebrae. *Biomed Res*. 2017;29:464-471.

16. Tao Y, Yunle W, Zong S, et al. Biomechanical characteristics of lumbar vertebra fixation based on finite element analysis. *Chinese Journal of Tissue Engineering Research*. 2016;20:1932-1938.

17. Yan JZ, Qiu GX, Wu ZH, Wang XS, Xing ZJ. Finite element analysis in adjacent segment degeneration after lumbar fusion. *Int J Med Robot*. 2011;7:96-100.

18. Anandjiwala J, Seo JY, Ha KY, Oh IS, Shin DC. Adjacent segment degeneration after instrumented posterolateral lumbar fusion: a prospective cohort study with a minimum five-year follow-up. *Eur Spine J*. 2011;20:1951-1960.

19. Chow DH, Luk KD, Evans JH, Leong JC. Effects of short anterior lumbar interbody fusion on biomechanics of neighboring unfused segments. *Spine (Phila Pa 1976)*. 1996;21:549-555.

20. Chen WJ, Lai PL, Tai CL, Chen LH, Niu CC. The effect of sagittal alignment on adjacent joint mobility after lumbar instrumentation–a biomechanical study of lumbar vertebrae in a porcine model. *Clin Biomech (Bristol, Avon)*. 2004;19:763-768.

21. Lee CK, Langrana NA. Lumbosacral spinal fusion. A biomechanical study. *Spine (Phila Pa 1976)*. 1984;9:574-581.

22. Xu H, Tang H, Guan X, et al. Biomechanical comparison of posterior lumbar interbody fusion and transforaminal lumbar interbody fusion by finite element analysis. *Neurosurgery*. 2013;72:21-26.

23. Iatridis JC, Setton LA, Weidenbaum M, Mow VC. Alterations in the mechanical behavior of the human lumbar nucleus pulposus with degeneration and aging. *J Orthop Res*. 1997;15:318-322.

24. Lee CK. Accelerated degeneration of the segment adjacent to a lumbar fusion. *Spine (Phila Pa 1976)*. 1988;13:375-377.

Conflict of interest statement: This work was supported by the Project of Scientific and Technological Innovation Team of Spinal Degeneration of Xianyang in 2014 (2014-8), the Research Fund of Provincial Health Department in 2016 (2016D071), and the Project of Xianyang Science and Technology Bureau in 2016 (2016K02-99).

Received 5 September 2018; accepted 21 November 2018

Citation: World Neurosurg. (2019) 124:e51-e57.
https://doi.org/10.1016/j.wneu.2018.11.195

Journal homepage: ***www.journals.elsevier.com/world-neurosurgery***

Available online: ***www.sciencedirect.com***

1878-8750/$ - see front matter